Human population dynamics in Europe over the Last Glacial Maximum

Miikka Tallavaara[a,1], Miska Luoto[b], Natalia Korhonen[c,d], Heikki Järvinen[d], and Heikki Seppä[b]

[a]Department of Philosophy, History, Culture and Art Studies, University of Helsinki, FI-00014 Helsinki, Finland; [b]Department of Geosciences and Geography, University of Helsinki, FI-00014 Helsinki, Finland; [c]Climate Change Research Unit, Finnish Meteorological Institute, FI-00101 Helsinki, Finland; and [d]Department of Physics, University of Helsinki, FI-00014 Helsinki, Finland

Edited by Jean-Pierre Bocquet-Appel, Ecole Pratique des Hautes Etudes, Paris, France, and accepted by the Editorial Board May 21, 2015 (received for review February 25, 2015)

The severe cooling and the expansion of the ice sheets during the Last Glacial Maximum (LGM), 27,000–19,000 y ago (27–19 ky ago) had a major impact on plant and animal populations, including humans. Changes in human population size and range have affected our genetic evolution, and recent modeling efforts have reaffirmed the importance of population dynamics in cultural and linguistic evolution, as well. However, in the absence of historical records, estimating past population levels has remained difficult. Here we show that it is possible to model spatially explicit human population dynamics from the pre-LGM at 30 ky ago through the LGM to the Late Glacial in Europe by using climate envelope modeling tools and modern ethnographic datasets to construct a population calibration model. The simulated range and size of the human population correspond significantly with spatiotemporal patterns in the archaeological data, suggesting that climate was a major driver of population dynamics 30–13 ky ago. The simulated population size declined from about 330,000 people at 30 ky ago to a minimum of 130,000 people at 23 ky ago. The Late Glacial population growth was fastest during Greenland interstadial 1, and by 13 ky ago, there were almost 410,000 people in Europe. Even during the coldest part of the LGM, the climatically suitable area for human habitation remained unfragmented and covered 36% of Europe.

hunter-gatherers | demography | niche modeling | climate change | Paleolithic

Growing populations of anatomically and behaviorally modern humans have been partly responsible for past ecosystem changes such as the extinctions of Pleistocene megafauna and Neanderthal humans (1, 2). In addition to the destiny of other species, human population size also influences our own cultural and genetic evolution. Large pools of interacting individuals can create and maintain adaptive skills, as well as phonological variation, more effectively than small populations, and they are also capable of faster cumulative cultural evolution (3–5). A decrease in population size may even result in a loss of complex cultural traits (6). The effects of population size on cultural variation are thus roughly similar to the effects of population size on genetic variation (7).

The study of the role of human population size in cultural and genetic evolution and past ecosystem changes necessitates estimates of population dynamics extending far beyond historical times. The archaeological record illustrates patterns of human population range and size dynamics (8–10), but it does not offer quantitative population size data. Archaeological reconstructions of population dynamics are also bound to the regions and time periods that offer a sufficiently rich archaeological record. In addition to archaeological data, information on past population patterns can be inferred from genetic data using skyline-plot methods (11) and pairwise or multiple sequentially Markovian coalescent analyzes (12, 13). However, these methods depend on estimates of DNA mutation rate and molecular clock calibrations, which are still debated (14, 15) and imprecise, leading to poor temporal resolution. Furthermore, these methods track changes in effective population size that does not have a straightforward relationship with the actual census population size (16). Together with poor resolution, this makes it extremely difficult to meaningfully compare DNA-based population reconstructions with the records of cultural or environmental changes.

Here, we take a different approach and model human population size and range dynamics in the last glacial Europe independently of archaeological and genetic data. Ethnographic studies have found a link between climate and the diet, mobility, and territory size of hunter-gatherers (17–20). We hypothesize that correlation exists also between climate and hunter-gatherer population density. We take advantage of this potential climate connection and use an approach made possible by recent developments in climate envelope modeling.

Climate envelope or niche models use associations between aspects of climate and the occurrences of species to estimate the conditions that are suitable for maintaining viable populations (21–23). By using information on how the climate affects modern hunter-gatherer population densities, this framework allows us to evaluate climatic suitability for humans and simulate their potential distribution and abundance under the changing climatic conditions of the last glacial, thus overcoming the above-mentioned limitations of approaches using only archaeological or genetic data. We use ethnographic data on terrestrially adapted mobile hunter-gatherers and their climatic space (24) (Dataset S1) to construct a calibration model that predicts hunter-gatherer presence and population density by three climatic predictors: potential evapotranspiration and water balance, both of which exert strong

Significance

Despite its importance for understanding genetic, cultural, and linguistic evolution, prehistoric human population history has remained difficult to reconstruct. We show that the dynamics of the human population in Europe from 30,000 to 13,000 y ago can be simulated using ethnographic and paleoclimate data within the climate envelope modeling approach. Correspondence between the population simulation and archaeological data suggests that population dynamics were indeed driven by major climate fluctuations, with population size varying between 130,000 and 410,000 people. Although climate has been an important determinant of human population dynamics, the climatic conditions during the last glacial were not as harsh as is often presented, because even during the coldest phases, the climatically suitable area for humans covered 36% of Europe.

Author contributions: M.T., M.L., and H.S. designed research; M.T., M.L., N.K., H.J., and H.S. performed research; M.T. and M.L. contributed new reagents/analytic tools; M.T., M.L., N.K., and H.J. analyzed data; and M.T., M.L., N.K., H.J., and H.S. wrote the paper.

The authors declare no conflict of interest.

This article is a PNAS Direct Submission. J.-P.B.-A. is a guest editor invited by the Editorial Board.

[1]To whom correspondence should be addressed. Email: miikka.tallavaara@gmail.com.

This article contains supporting information online at www.pnas.org/lookup/suppl/doi:10.1073/pnas.1503784112/-/DCSupplemental.

influence on ecosystem productivity and species richness, and the mean temperature of the coldest month that affects wintering conditions, such as winter mortality (25, 26). This model is extrapolated over the European landscape for 30–13 ky ago using climate predictor values obtained by statistical downscaling of the CLIMBER-2 climate model simulation data (27, 28) (Dataset S2). The period in question was chosen because it extends from the end of the Marine Isotope Stage 3 (MIS-3) to the Last Glacial Termination and includes the coldest phase and the largest ice sheet extent of the last glaciation (29).

In practice, estimates of absolute prehistoric population size or density cannot be truly verified with any existing data. Because our model is not archaeologically informed, it is, however, possible to use the dataset of archaeological radiocarbon dates (30) (Dataset S3) to evaluate the simulated spatial and temporal patterns and, in that sense, the realism of our simulation. Such archaeological data are increasingly used as a proxy in studies of prehistoric human population dynamics (8–10, 31, 32).

Results

Fig. 1 shows that the temporal patterns in the simulated population size and archaeological population proxy are remarkably consistent (r_P = 0.84, P < 0.00002). Both show relatively high late-MIS-3 population size levels, a decline toward the Last Glacial Maximum (LGM) minimum, and a rapid growth during the Late Glacial. The simulation suggests that the human population size in Europe was about 330,000 at 30 ky ago, 130,000 during its minimum at 23 ky ago, and almost 410,000 at 13 ky ago, during the Greenland interstadial 1. The mean population density in the inhabited area varied between 2.8 and 5.1 persons per 100 km^2.

The simulated spatial pattern of human population (Figs. 2 and 3) indicates a population contraction starting in line with the ice sheet expansion at 27 ky ago. During the peak LGM, the northern limit of contiguous population in Europe extended from central France to lowlands in southern Germany and to the southern parts of modern Ukraine and European Russia (Fig. 2). Thus, there was an uninhabited zone about 500 km wide between the ice sheet and the northern limit of the human population. However, our simulation suggests that the continuously suitable and inhabited area between 30 and 13 ky ago covered 36% of the European land area even during the coldest LGM, stretching to the north of the Alps (Fig. 3), a result supported also by an emerging archaeological picture (33). In addition, the simulation shows a persistent southwest-northeast gradient of decreasing population densities, with the densest populations throughout the LGM in the Iberian Peninsula and the Mediterranean region (Figs. 2 and 3). The post-LGM recolonization of the continent began at 19 ky ago.

These spatial dynamics concur with the archaeological data, although the latter show a spatially and temporally more sporadic pattern. Such a sparse pattern is most probably a result of a Wallacean shortfall-like effect of incomplete information on species distribution. Although Wallacean shortfall is true for current plant and animal species, paleontological and archaeological records provide obviously even more incomplete and coarse reflection of true ranges (23).

There are, nevertheless, two instances where the simulated range and density of the human population deviate from the distribution of archaeological data. First, in northern Russia, the archaeological record indicates occasional presence of humans much farther north than our simulation suggests. These anomalies may represent human populations whose climatic tolerance differed from that of the modern hunter-gatherer populations used in the calibration model, because it has been suggested that the archaeological lithic assemblage of Byzovaya site in the Polar Urals was produced by Neanderthals (34). The presence of Neanderthals is controversial (35), however, and the anomalies continue sporadically throughout the LGM, when Neanderthals

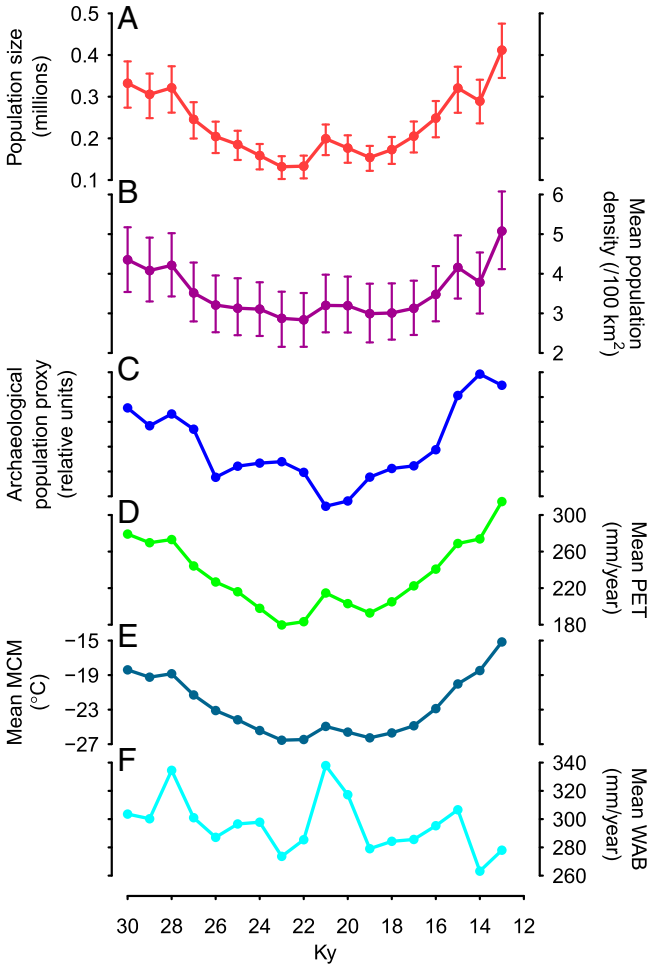

Fig. 1. Comparisons between simulated hunter-gatherer population size and density, the archaeological population proxy, and paleoclimatic simulations between 30 and 13 ky ago in Europe. (*A*) Simulated human population size in Europe. Error bars show the resampling-based confidence limits (95%). (*B*) Simulated mean density in the inhabited area of Europe. Error bars show the resampling-based confidence limits (95%). (*C*) Archaeological population size proxy based on the taphonomically corrected number of dates. (*D*) European mean of simulated potential evapotranspiration. (*E*) European mean of simulated mean temperature of the coldest month. (*F*) European mean of simulated water balance. *D*–*F* are based on the downscaling from the CLIMBER-2 climate model.

are assumed to have already been extinct. Nonetheless, our results allow for the possibility that the late MIS-3 populations in northern Russia were biologically or behaviorally different from later humans.

Second, whereas our model simulates high population densities in the Mediterranean region, the density of archaeological data in the region is relatively low throughout the study period. This difference does not relate to the properties of the climate data used in the simulation, because the LGM snapshot population simulations based on state-of-the-art general circulation model data (36–38) show the same pattern (Fig. S1). This similarity of the patterns strongly suggests that the Iberian Peninsula and the Mediterranean region have indeed been climatically the most suitable areas for hunter-gatherers throughout the LGM.

It is possible that some nonclimatic factors made the region less suitable for humans, which would explain the difference between the simulation based on the hunter-gatherer climatic envelope and the archaeological data. For example, the climatically highly

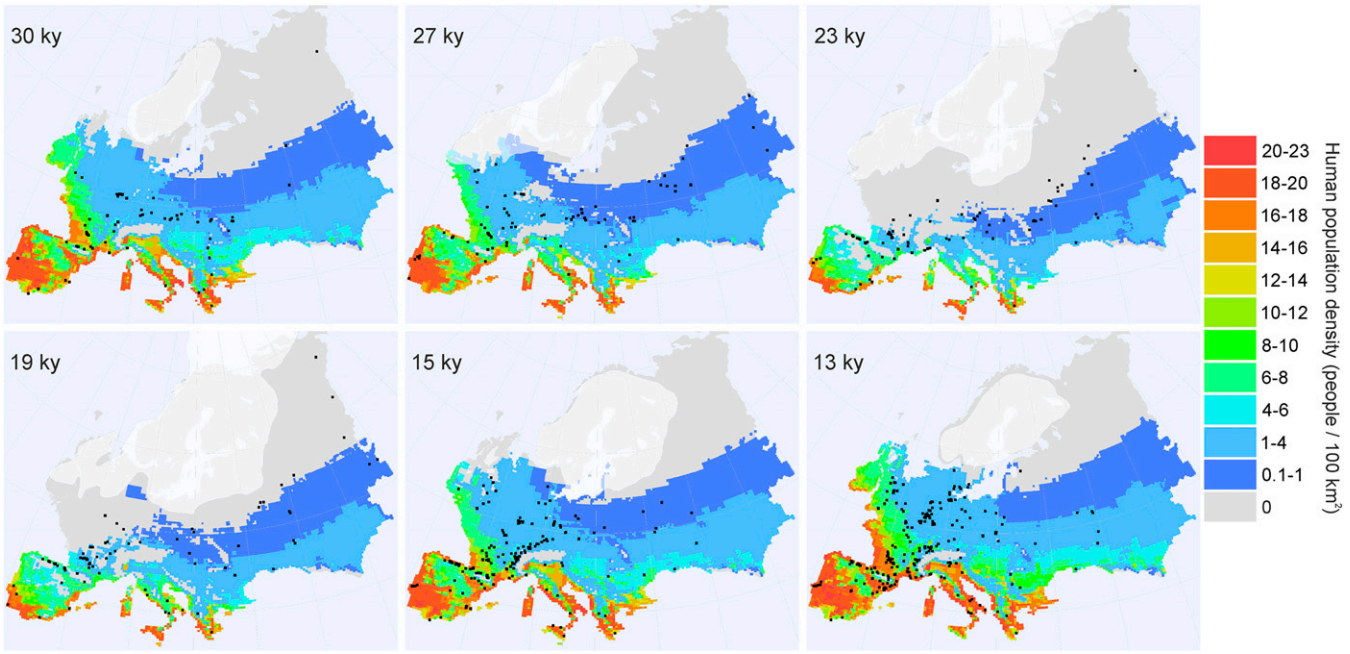

Fig. 2. Simulated human population range and density compared with the spatial distribution of archaeological sites during six time intervals from 30 to 13 ky ago. Archaeological sites are indicated with black dots and in each time slice they represent sites dated within 1,000-y bins.

suitable, but relatively small, island of Sardinia may not have been attractive for terrestrially adapted hunter-gatherer groups of the LGM Europe. On a larger scale, however, the spatial distribution of archaeological data may not adequately reflect the distribution of human population, because of the systematic differences in taphonomic processes between different parts of Europe. Due to a combination of climatic and topographic features, erosion rates are higher in the Mediterranean region than in other parts of Europe (39, 40). The high erosion leads to loss or disturbance of the sediment layers containing archaeological material, which may explain the relatively low density of radiocarbon dated sites in the Mediterranean region. For example, in a sample of 164 Middle Paleolithic sites in southern Iberia, almost 80% of the sites were found to be clearly in a secondary context (41).

Research history may also play role in the spatial variability of archaeological data. In Portugal, for instance, there were only four Upper Paleolithic sites known in the early 1960s, and the region was considered largely uninhabited (42). Sensitivity of archaeological distributions to changes in research interests is reflected by the fact that in 50 y the number of sites has multiplied manifold with such discoveries as the Côa Valley dwelling and rock art sites (43, 44). However, relatively few of these new sites have been radiocarbon dated (44) and would not show up in our archaeological proxy. It is thus likely that the discrepancy between the simulated population densities and the spatial distribution of archaeological data in the Mediterranean region is a result of combined effect of research history and erosion-induced taphonomic loss and disturbance of archaeological material. In general, the archaeological data, nevertheless, fall within the simulated range area and the northern limits of the simulation and the archaeological data correspond to each other relatively well.

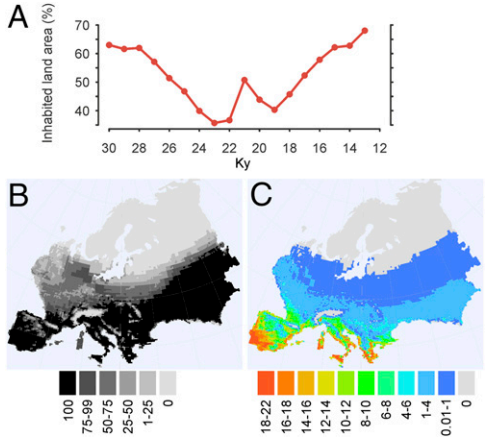

Fig. 3. Climatic suitability of Europe for human population over the LGM according to the simulation. (*A*) Changes in the percentage of potentially inhabited land area in Europe. (*B*) Percentage of time the area has potentially been inhabited between 30 and 13 ky ago. (*C*) Mean population density (people/100 km^2) between 30 and 13 ky ago.

Discussion

The overall similarity of the simulated and archaeological population patterns supports our results about the European human population changes between 30 and 13 ky ago. However, the simulated population size in LGM Europe appears extremely high compared with the results of Bocquet-Appel et al. (45), who estimated the population size to be less than 6,000 persons. There are two main reasons that lead to these considerably smaller population size estimates. First, Bocquet-Appel et al. (45) estimate the human population range from the spatial distribution of archaeological data while assuming that it adequately reflects the true range of the human population. As discussed above, this assumption is probably not valid, because archaeological remains provide an incomplete and coarse reflection of past geographical distributions of human activity. Second, compared with ethnographically known hunter-gatherer populations (17, 24), Bocquet-Appel et al. (45) use extremely low population density estimates and, even more importantly, only single estimates for each period in question, which does not take into account geographical variability in climate

and environment. As our simulation shows, this variability has a strong impact on human population densities and this result appears to be robust with respect to the choice of climate model simulation data (Fig. S1).

In addition, the simulated temporal pattern in population size and density differs from many previous reconstructions of Pleistocene dynamics of European populations, especially those based on DNA data (11–13), which show monotonic growth for the last 50 ky. However, the monotonic growth does not match the archaeological record, which shows substantial variations in human population size at high and low frequencies. These variations seem often to follow climatic variability and, as shown here, they are also simulated with the climate envelope modeling.

Our results have three important implications. First, we show that the range and size of prehistoric hunter-gatherer populations can be realistically modeled using information on modern hunter-gatherers and paleoclimatic simulations. This climate envelope modeling approach provides valuable insights into the patterns and causes of long-term human population dynamics and a necessary complement to archaeological and DNA-based methods when studying prehistoric human demography. Second, the consistency between the simulated patterns and the archaeological data are remarkable because it suggests that climatic conditions were crucial drivers of last glacial human population dynamics. This consistency also indicates that the climate envelope of the hunter-gatherers has remained relatively constant from the last glacial to present. Millennia of cultural evolution have not fundamentally changed constraints on terrestrially adapted hunter-gatherer populations posed by the climate. Third, even the harsh conditions of the LGM sustained a substantial human population in Europe, which was not fragmented to totally isolated refugia. The continuous range would have facilitated a flow of genes and cultural information between the western and eastern parts of the continent, which, in turn, has implications for understanding genetic diversity and cultural evolution in Europe.

Materials and Methods

Constructing the Calibration Model. We used an ethnographic dataset ($n = 339$) of modern and recent historical hunter-gatherer populations (24) to extract calibration data to train the statistical models. This dataset is obviously geographically biased. The spatial distribution of ethnographically documented hunter-gatherers does not reflect the geographical area that is suitable for hunter-gatherers, because large areas previously occupied by foragers are dominated by agricultural populations from the Mid-Holocene onward. However, it has been shown that the ethnographic sample of hunter-gatherers is not biased in terms of their niche space (24). Therefore, these data are suitable for niche modeling including climate envelope modeling that are extrapolated to the geographical areas not recently occupied by hunter-gatherers.

For the calibration data, we excluded cases where subsistence is based on mutualistic relations with non–hunter-gatherers (SUBPOP = X). Because the isotope studies of human bone collagen indicate that the Pleistocene hunter-gatherers obtained, at most, 30% of their dietary protein from aquatic resources (46, 47), we also excluded populations whose main livelihood comes from aquatic resources (SUBSP = 3). In addition, we excluded populations that used horses (SYSTATE3 = 1), because mounted hunter-gatherers are unknown in the European Paleolithic record. To keep the simulated population densities conservative, we excluded populations that either move into and out of a central location that is maintained for more than 1 y or are completely sedentary (GRPPAT = 2). These groups usually live under high population densities. The exclusion means that the simulation assumes that the Pleistocene human populations in Europe were residentially mobile, an assumption commonly held by archaeologists. For a comparison, we present in *SI Text* and Fig. S2 a more relaxed simulation based on the calibration data that includes also semi- and fully sedentary groups.

Altogether, the calibration data includes information on 127 hunter-gatherer populations. Because this dataset gives information only on environments where the hunter-gatherers have existed in recent historical times, we added 120 pseudo-absence data points to the climate space where terrestrially adapted hunter-gatherers have not recently existed (e.g., extremely cold and extremely hot and dry) to enhance the performance of the statistical models (Fig. S3 and Dataset S1). Pseudo-absence data have information on climatic conditions and the hunter-gatherer density for each point is zero. The climate data for these points were obtained from the WorldClim database (48). Addition of pseudo-absence data to presence-only data are a standard procedure in ecological modeling (49, 50).

We used potential evapotranspiration (PET), water balance (WAB), and mean temperature of the coldest month (MCM) as predictors of the density (DENSITY) and presence/absence (DENSITY > 0) of the human population. PET and MCM values are directly available from the ethnographic dataset. WAB values were calculated as the difference between annual precipitation and PET.

To model the distribution and density of the human population, we used two frameworks: one predicting the range (presence/absence) of the human population and the other predicting population density. The human population occurrence was modeled as a binary response variable and density as a continuous response variable. To take into account the fact that different modeling algorithms give diverse predictions, the following six alternative techniques were used to relate human presence/absence and density with the explanatory climatic variables: generalized linear modeling (GLM) (51), generalized additive modeling (GAM) (52), support vector machines (SVM) (53, 54), classification tree analysis (CTA) (55, 56), random forest (RF) (57, 58), and generalized boosting methods (GBM) (59, 60). All of the methods were implemented using R statistical software (61). A more detailed description of these techniques is given in the *SI Text*.

Predicted probabilities of occurrence were converted to presence/absence predictions using the threshold value maximizing the sum of sensitivity and specificity (62) (*SI Text*).

The ability of the models to predict human population occurrence and density was assessed using cross-validation (70% random sample for calibration and 30% for validation; 500 repeats). The predictive power of the binary models was determined by testing the accuracy of predictions made for the validation dataset by calculating the area under the curve of a receiver operating characteristic plot (AUC) and the true skill statistic (TSS) (63). For density models, mean R^2 values were calculated. Predictive accuracies of the six models based on three climate variables are summarized in Table S1.

To further evaluate the ability of climate envelope modeling approach to correctly simulate hunter-gatherer populations, we simulated Australian hunter-gatherer population at 0.5 ky ago and compared the result to the historical, ethnographic, and archaeological estimates of population size at the European contact (64–66). This simulation is presented in the supplement (*SI Text* and Fig. S4).

Climate Model. The monthly average temperature and annual precipitation values for Europe were generated using a full last glacial cycle simulation (126 ky ago until the present day) with the CLIMBER-2-SICOPOLIS model system (27) that simulates climate at a temporal resolution of 1,000 y. Climate data were downscaled here to the resolution of 1.5° (longitude) × 0.75° (latitude) for a time slice of 30–13 ky ago using a GAM (52). The GAM used here was calibrated (28) using observations of the recent past climate (67, 68) and a short time slice simulation of the LGM (about 22 ky ago) using a relatively high-resolution general circulation model (CCSM4) (36). See *SI Text* for details. The temperature data at the spatial resolution of 1.5° × 0.75° were regridded to 0.375° × 0.250°. During the regridding process, monthly temperature values were lapsed by the pseudo adiabatic lapse rate (6.4 °C/km) to account for differences in average elevation between the fine-scale and coarse-scale grids (69) (Dataset S2). The problem with the climate model is that it cannot trace high-frequency climate variations. Therefore, for example, some of the cold events, such as Heinrich 1, do not show up in the model data.

Human Population Range and Density Model. The range of the human population for every 1,000 y between 30 and 13 ky ago was simulated by predicting presence/absence of humans for every 0.375° × 0.25° cell containing land area. This simulation was done by using the above-mentioned calibration model algorithms and climate predictor values derived from the climate simulation. The climate simulation based monthly average temperature, and annual precipitation values were used to calculate PET and WAB values. WAB was calculated as the difference between precipitation and potential evapotranspiration. PET was calculated as (70, 71)

$$\mathrm{PET} = 58.93 \times \mathrm{T}_{\mathrm{above\ 0\ °C}}$$

The results of different model algorithms were averaged by using ensemble averaging methods that have been shown to remarkably increase the robustness of forecasts (72). For binary models, majority vote was used. Majority vote is an ensemble forecasting method that assigns a presence prediction only when more than half of the models (i.e., >3) predicts a presence (73).

Next, population density was predicted for every 0.375° × 0.25° cell inside the modeled range. For density models, to average the results based on different algorithms, their median was calculated (consensus method) (72) for each cell.

To calculate the human population size in Europe every 1,000 y, we first calculated the land area of each cell. Here we took into account the systematic areal change of the 0.375° × 0.25° cells and the actual percentage of the land area in each cell. Next, we multiplied the predicted population density of the cell by the land area of the cell and summed these values to get the total population size.

To evaluate the uncertainty of population size estimates, we repeated the whole process from calibration model fitting to calculation of population size 500 times using each time a random sample (70%) of the training/calibration data. This procedure allowed us to calculate confidence limits for the simulated population size estimates. The set of modeling techniques and climate data were held constant throughout the process.

The changes in the percentage of inhabited land area in Europe between 30 and 13 ky ago were calculated by relating the summed land area of the inhabited cells to the total land area of the cells containing land (ice sheet included). To estimate the percentage of time the cell has been inhabited between 30 and 13 ky ago, we counted the number of 1,000-y intervals when the cell was inhabited (maximum 18) and related this to the total number of time intervals.

The ice sheets shown in Fig. 2 were drawn according to four sources (74–77). There is some overlap between the reconstructed ice sheets and the modeled population range, especially in the British Isles at 27 ky ago. This overlap may partly be due to the generalizing effect of using 1,000-y time intervals in climate and human population simulations and in the ice sheet reconstructions but may also reflect some inaccuracies in the modeled human populations ranges and/or ice sheet reconstructions.

We have taken into account eustatic changes in the sea level and the consequent changes in the land area of Europe by adjusting the sea level according to a global sea level change curve (78).

Archaeological Human Population Proxy. Previous approaches of prehistoric human distribution and niche modeling have trained the predictive models using archaeological site distribution data (79–81). By keeping our calibration model independent from the archaeological data, we are able to test our simulation with the archaeological data.

To evaluate the simulated human population range and density, they were compared with the archaeological population proxy. The population proxy is based on ^{14}C dates, and the dates extracted from the International Union for Quaternary Science (INQUA) Radiocarbon Paleolithic Europe Database v12 form the backbone of data (30). We also included several dates from other recently published sources. The reasoning behind such a dates-as-data approach is that reliable archaeological radiocarbon dates indicate human presence in the area and that the temporal variation in the frequencies of ^{14}C dates reflects changes in prehistoric population size (8–10, 31, 32, 82).

The dataset was critically evaluated using the information given in the INQUA database. We excluded (*i*) all dates that were qualified as unreliable or contaminated, (*ii*) dates without coordinates or laboratory reference, (*iii*) duplicate dates, (*iv*) dates with SEs greater than 5% of the mean ^{14}C age, (*v*) dates from gyttja, humus, peat, soil or soil organics, organic sediment, humic acid fraction of the sediment, and fossil timber, (*vi*) dates of marine origin, such as shell, marine shell, and molluscs, (*vii*) dates without a clear link to human activity, such as terminus ante and post quem, surface, above, up from, top, below and beneath of the cultural layer(s), minimum or maximum age of the layer, and beyond site, and (*viii*) dates of cave bear (*Ursus spelaeus*). In some cases, coordinates or even ages were corrected according to the original publication of the date. After the cleaning, the dataset contains 3,718 ^{14}C dates from 895 sites (Dataset S3).

The dates were calibrated using the OxCal 4.2 calibration program (83) and IntCal13 calibration curve (84). In the analyses, we used the calibrated median dates. For comparisons between the model and archaeological data, median dates were grouped in intervals of 1,000 y so that the modeled human range at 30 ky was compared with the spatial distribution of dates between 30,499 and 29,500 cal BP, the modeled range at 29,000 cal BP to the distribution of dates between 29,499 and 28,500 cal BP, and so forth.

Surovell et al. (31) argued that the younger findings are overrepresented relative to older findings in the archaeological record due to the time-dependent influence of destructive processes such as erosion and weathering. Similar time-dependent loss processes seem to affect geological and palaeontological data, as well as historical coin records (85, 86). Therefore, the temporal frequency distributions should be corrected for this taphonomic bias. Surovell et al. (31) proposed a model of taphonomic bias and suggested how to use it to correct the temporal frequency distributions. This method was evaluated, modified, and implemented in several subsequent studies (1, 32, 82, 86). Here, we used a taphonomic bias model modified by Williams (32). The temporal distribution of the taphonomically corrected number of dates was used as a proxy for relative changes in human population size between 30 and 13 ky ago, and this distribution was compared with the temporal distribution of modeled population sizes. See Fig. S5 for the comparison between raw temporal frequency distribution and the taphonomically corrected temporal frequency distribution of archaeological dates.

ACKNOWLEDGMENTS. We thank A. Lister, M. Fortelius, T. Rankama, H. Renssen, and F. Riede for discussions and comments on an earlier version of the manuscript; A. Ganopolski for providing the climate simulations of CLIMBER-2-SICOPOLIS; and W. Perttola for technical help with spatial analyses. M.T. acknowledges financial support from the Kone Foundation.

1. Lorenzen ED, et al. (2011) Species-specific responses of Late Quaternary megafauna to climate and humans. *Nature* 479(7373):359–364.
2. Mellars P, French JC (2011) Tenfold population increase in Western Europe at the Neandertal-to-modern human transition. *Science* 333(6042):623–627.
3. Derex M, Beugin M-P, Godelle B, Raymond M (2013) Experimental evidence for the influence of group size on cultural complexity. *Nature* 503(7476):389–391.
4. Powell A, Shennan S, Thomas MG (2009) Late Pleistocene demography and the appearance of modern human behavior. *Science* 324(5932):1298–1301.
5. Bromham L, Hua X, Fitzpatrick TG, Greenhill SJ (2015) Rate of language evolution is affected by population size. *Proc Natl Acad Sci USA* 112(7):2097–2102.
6. Henrich J (2004) Demography and cultural evolution: How adaptive cultural processes can produce maladaptive losses: The Tasmanian case. *Am Antiq* 69(2):197–214.
7. Frankham R (1996) Relationship of genetic variation to population size in wildlife. *Conserv Biol* 10(6):1500–1508.
8. Gamble C, Davies W, Pettitt P, Hazelwood L, Richards M (2005) The archaeological and genetic foundations of the European population during the Late Glacial: Implications for "agricultural thinking." *Camb Archaeol J* 15(02):193–223.
9. Steele J (2010) Radiocarbon dates as data: Quantitative strategies for estimating colonization front speeds and event densities. *J Archaeol Sci* 37(8):2017–2030.
10. Shennan S, et al. (2013) Regional population collapse followed initial agriculture booms in mid-Holocene Europe. *Nat Commun* 4:2486.
11. Atkinson QD, Gray RD, Drummond AJ (2008) mtDNA variation predicts population size in humans and reveals a major Southern Asian chapter in human prehistory. *Mol Biol Evol* 25(2):468–474.
12. Li H, Durbin R (2011) Inference of human population history from individual whole-genome sequences. *Nature* 475(7357):493–496.
13. Schiffels S, Durbin R (2014) Inferring human population size and separation history from multiple genome sequences. *Nat Genet* 46(8):919–925.
14. Scally A, Durbin R (2012) Revising the human mutation rate: Implications for understanding human evolution. *Nat Rev Genet* 13(10):745–753.
15. Fu Q, et al. (2013) A revised timescale for human evolution based on ancient mitochondrial genomes. *Curr Biol* 23(7):553–559.
16. Hawks J (2008) From genes to numbers: Effective population sizes in human evolution. *Recent Advances in Palaeodemography*, ed Bocquet-Appel J-P (Springer, Dordrecht, The Netherlands), pp 9–30.
17. Kelly RL (2013) *The Lifeways of Hunter-Gatherers: The Foraging Spectrum* (Cambridge Univ Press, Cambridge, UK), 2nd Ed.
18. Binford LR (1980) Willow smoke and dogs' tails: Hunter-gatherer settlement systems and archaeological site formation. *Am Antiq* 45(1):4–20.
19. Birdsell JB (1953) Some environmental and cultural factors influencing the structuring of Australian aboriginal populations. *Am Nat* 87(834):171–207.
20. Hamilton MJ, Burger O, Walker RS (2012) Human ecology. *Metabolic Ecology*, eds Sibly RM, Brown JH, Kodric-Brown A (John Wiley & Sons, Chichester, UK), pp 248–257.
21. Pearson RG, Dawson TP (2003) Predicting the impacts of climate change on the distribution of species: Are bioclimate envelope models useful? *Glob Ecol Biogeogr* 12(5):361–371.
22. Araújo MB, Peterson AT (2012) Uses and misuses of bioclimatic envelope modeling. *Ecology* 93(7):1527–1539.
23. Svenning J-C, Fløjgaard C, Marske KA, Nógues-Bravo D, Normand S (2011) Applications of species distribution modeling to paleobiology. *Quat Sci Rev* 30(21-22):2930–2947.
24. Binford LR (2001) *Constructing Frames of Reference: An Analytical Method for Archaeological Theory Building Using Ethnographic and Environmental Data Sets* (Univ of California Press, Berkeley).
25. Currie DJ (1991) Energy and large-scale patterns of animal- and plant-species richness. *Am Nat* 137(1):27–49.
26. Franklin J (2010) *Mapping Species Distributions: Spatial Inference and Prediction* (Cambridge Univ Press, Cambridge, UK).
27. Ganopolski A, Calov R, Claussen M (2010) Simulation of the last glacial cycle with a coupled climate ice-sheet model of intermediate complexity. *Clim Past* 6(2):229–244.
28. Korhonen N, Venäläinen A, Seppä H, Järvinen H (2014) Statistical downscaling of a climate simulation of the last glacial cycle: Temperature and precipitation over Northern Europe. *Clim Past* 10(4):1489–1500.
29. Clark PU, et al. (2009) The Last Glacial Maximum. *Science* 325(5941):710–714.
30. Vermeersch PM (2005) European population changes during Marine Isotope Stages 2 and 3. *Quat Int* 137(1):77–85.

31. Surovell TA, Byrd Finley J, Smith GM, Brantingham PJ, Kelly R (2009) Correcting temporal frequency distributions for taphonomic bias. *J Archaeol Sci* 36(8):1715–1724.
32. Williams AN (2012) The use of summed radiocarbon probability distributions in archaeology: A review of methods. *J Archaeol Sci* 39(3):578–589.
33. Terberger T, Street M (2002) Hiatus or continuity? New results for the question of pleniglacial settlement in Central Europe. *Antiquity* 76(293):691.
34. Slimak L, et al. (2011) Late Mousterian persistence near the Arctic Circle. *Science* 332(6031):841–845.
35. Zwyns N, Roebroeks W, McPherron SP, Jagich A, Hublin J-J (2012) Comment on "Late Mousterian persistence near the Arctic Circle". *Science* 335(6065):167.
36. Gent PR, et al. (2011) The community climate system model, version 4. *J Clim* 24(19): 4973–4991.
37. Giorgetta MA, et al. (2013) Climate and carbon cycle changes from 1850 to 2100 in MPI-ESM simulations for the Coupled Model Intercomparison Project phase 5. *J Adv Model Earth Syst* 5(3):572–597.
38. Watanabe S, et al. (2011) MIROC-ESM 2010: Model description and basic results of CMIP5-20c3m experiments. *Geosci Model Dev* 4(4):845–872.
39. Vanmaercke M, Poesen J, Verstraeten G, de Vente J, Ocakoglu F (2011) Sediment yield in Europe: Spatial patterns and scale dependency. *Geomorphology* 130(3-4):142–161.
40. Poesen JWA, Hooke JM (1997) Erosion, flooding and channel management in Mediterranean environments of southern Europe. *Prog Phys Geogr* 21(2):157–199.
41. Jennings R, Finlayson C, Fa D, Finlayson G (2011) Southern Iberia as a refuge for the last Neanderthal populations. *J Biogeogr* 38(10):1873–1885.
42. Roche J (1964) Le Paléolithique supérieur portugais. Bilan de nos connaissances et problèmes. *Bull Société Préhistorique Fr Études Trav* 61(1):11–27.
43. Aubry T, Llach XM, Sampaio JD, Sellami F (2002) Open-air rock-art, territories and modes of exploitation during the Upper Palaeolithic in the Côa Valley (Portugal). *Antiquity* 76(291):62–76.
44. Aubry T, Luís L, Mangado Llach J, Matias H (2012) We will be known by the tracks we leave behind: Exotic lithic raw materials, mobility and social networking among the Côa Valley foragers (Portugal). *J Anthropol Archaeol* 31(4):528–550.
45. Bocquet-Appel J-P, Demars P-Y, Noiret L, Dobrowsky D (2005) Estimates of Upper Palaeolithic meta-population size in Europe from archaeological data. *J Archaeol Sci* 32(11):1656–1668.
46. Richards MP, Pettitt PB, Stiner MC, Trinkaus E (2001) Stable isotope evidence for increasing dietary breadth in the European mid-Upper Paleolithic. *Proc Natl Acad Sci USA* 98(11):6528–6532.
47. Drucker D, Bocherens H (2004) Carbon and nitrogen stable isotopes as tracers of change in diet breadth during Middle and Upper Palaeolithic in Europe. *Int J Osteoarchaeol* 14(3-4):162–177.
48. Hijmans RJ, Cameron SE, Parra JL, Jones PG, Jarvis A (2005) Very high resolution interpolated climate surfaces for global land areas. *Int J Climatol* 25(15):1965–1978.
49. Phillips SJ, et al. (2009) Sample selection bias and presence-only distribution models: Implications for background and pseudo-absence data. *Ecol Appl* 19(1):181–197.
50. Barbet-Massin M, Jiguet F, Albert CH, Thuiller W (2012) Selecting pseudo-absences for species distribution models: How, where and how many? *Methods Ecol Evol* 3(2):327–338.
51. McCullagh P, Nelder JA (1989) *Generalized Linear Models* (Chapman & Hall/CRC, Boca Raton, FL).
52. Hastie T, Tibshirani R (1990) *Generalized Additive Models* (Chapman & Hall/CRC, Boca Raton, FL).
53. Cortes C, Vapnik V (1995) Support-vector networks. *Mach Learn* 20(3):273–297.
54. Drucker H, Burges CJC, Kaufman L, Smola AJ, Vapnik V (1997) Support vector regression machines. *Advances in Neural Information Processing Systems 9*, eds Mozer MC, Jordan MI, Petsche T (MIT Press, Cambridge, MA), pp 155–161.
55. Breiman L, Friedman J, Stone CJ, Olshen RA (1984) *Classification and Regression Trees* (Chapman and Hall/CRC, New York), 1st Ed.
56. Venables WN, Ripley BD (2010) *Modern Applied Statistics with S* (Springer, New York), 4th Ed.
57. Breiman L (2001) Random forests. *Mach Learn* 45(1):5–32.
58. Prasad A, Iverson L, Liaw A (2006) Newer classification and regression tree techniques: Bagging and random forests for ecological prediction. *Ecosystems (N Y)* 9(2):181–199.
59. Ridgeway G (1999) The state of boosting. *Comput Sci Stat* 31:172–181.
60. Elith J, Leathwick JR, Hastie T (2008) A working guide to boosted regression trees. *J Anim Ecol* 77(4):802–813.
61. R Development Core Team (2014) *R: A Language and Environment for Statistical Computing* (R Foundation for Statistical Computing, Vienna).
62. Liu C, Berry PM, Dawson TP, Pearson RG (2005) Selecting thresholds of occurrence in the prediction of species distributions. *Ecography* 28(3):385–393.
63. Allouche O, Tsoar A, Kadmon R (2006) Assessing the accuracy of species distribution models: Prevalence, kappa and the true skill statistic (TSS): Assessing the accuracy of distribution models. *J Appl Ecol* 43(6):1223–1232.
64. White JP, Mulvaney DJ (1987) How many people? *Australians to 1788*, eds Mulvaney DJ, White JP (Fairfax, Syme & Weldon Associates, Broadway, Australia), pp 114–117.
65. Mulvaney DJ, Kamminga J (1999) *Prehistory of Australia* (Allen & Unwin, St Leonards, Australia).
66. Williams AN (2013) A new population curve for prehistoric Australia. *Proc R Soc B Biol Sci* 280(1761):20130486.
67. Mitchell TD, Jones PD (2005) An improved method of constructing a database of monthly climate observations and associated high-resolution grids. *Int J Climatol* 25(6):693–712.
68. Xie P, Arkin PA (1997) Global precipitation: A 17-year monthly analysis based on gauge observations, satellite estimates, and numerical model outputs. *Bull Am Meteorol Soc* 78(11):2539–2558.
69. Vajda A, Venäläinen A (2003) The influence of natural conditions on the spatial variation of climate in Lapland, northern Finland. *Int J Climatol* 23(9):1011–1022.
70. Skov F, Svenning J-C (2004) Potential impact of climatic change on the distribution of forest herbs in Europe. *Ecography* 27(3):366–380.
71. Holdridge LR (1967) *Life Zone Ecology* (Tropical Science Center, San Jose, Costa Rica).
72. Araújo MB, New M (2007) Ensemble forecasting of species distributions. *Trends Ecol Evol* 22(1):42–47.
73. Gallien L, Douzet R, Pratte S, Zimmermann NE, Thuiller W (2012) Invasive species distribution models – how violating the equilibrium assumption can create new insights. *Glob Ecol Biogeogr* 21(11):1126–1136.
74. Boulton G, Dongelmans P, Punkari M, Broadgate M (2001) Palaeoglaciology of an ice sheet through a glacial cycle: The European ice sheet through the Weichselian. *Quat Sci Rev* 20(4):591–625.
75. Clark CD, Hughes ALC, Greenwood SL, Jordan C, Sejrup HP (2012) Pattern and timing of retreat of the last British-Irish Ice Sheet. *Quat Sci Rev* 44:112–146.
76. Lambeck K, Purcell A, Zhao J, Svensson N-O (2010) The Scandinavian Ice Sheet: From MIS 4 to the end of the Last Glacial Maximum. *Boreas* 39(2):410–435.
77. Svendsen JI, et al. (2004) Late Quaternary ice sheet history of northern Eurasia. *Quat Sci Rev* 23(11–13):1229–1271.
78. Peltier WR, Fairbanks RG (2006) Global glacial ice volume and Last Glacial Maximum duration from an extended Barbados sea level record. *Quat Sci Rev* 25(23–24):3322–3337.
79. Banks WE, et al. (2008) Human ecological niches and ranges during the LGM in Europe derived from an application of eco-cultural niche modeling. *J Archaeol Sci* 35(2):481–491.
80. Banks WE, et al. (2011) Eco-cultural niches of the Badegoulian: Unraveling links between cultural adaptation and ecology during the Last Glacial Maximum in France. *J Anthropol Archaeol* 30(3):359–374.
81. Beeton TA, Glantz MM, Trainer AK, Temirbekov SS, Reich RM (2014) The fundamental hominin niche in late Pleistocene Central Asia: A preliminary refugium model. *J Biogeogr* 41(1):95–110.
82. Kelly RL, Surovell TA, Shuman BN, Smith GM (2013) A continuous climatic impact on Holocene human population in the Rocky Mountains. *Proc Natl Acad Sci USA* 110(2):443–447.
83. Bronk Ramsey C (2009) Bayesian analysis of radiocarbon dates. *Radiocarbon* 51(1): 337–360.
84. Reimer PJ, et al. (2013) IntCal13 and Marine13 radiocarbon age calibration curves 0–50,000 years cal BP. *Radiocarbon* 55(4):1869–1887.
85. Surovell TA, Brantingham PJ (2007) A note on the use of temporal frequency distributions in studies of prehistoric demography. *J Archaeol Sci* 34(11):1868–1877.
86. Peros MC, Munoz SE, Gajewski K, Viau AE (2010) Prehistoric demography of North America inferred from radiocarbon data. *J Archaeol Sci* 37(3):656–664.
87. Wood SN (2011) Fast stable restricted maximum likelihood and marginal likelihood estimation of semiparametric generalized linear models. *J R Stat Soc Series B Stat Methodol* 73(1):3–36.
88. Meyer D, Dimitriadou E, Hornik K, Weingessel A, Leisch F (2014) e1071: Misc Functions of the Department of Statistics (e1071), TU Wien. R package version 1.6-4. Available at CRAN.R-project.org/package=e1071. Accessed May, 2014.
89. Therneau T, Atkinson B, Ripley B (2014) rpart: Recursive partitioning and regression trees, R package version 4.1-8. Available at CRAN.R-project.org/package=rpart. Accessed May, 2014.
90. Liaw A, Wiener M (2002) Classification and regression by randomForest. *R News* 2(3): 18–22.
91. Friedman JH (2001) Greedy function approximation: A gradient boosting machine. *Ann Stat* 29(5):1189–1232.
92. VanDerWal J, Falconi L, Januchowski S, Shoo L, Storlie C (2014) SDMTools: Species Distribution Modelling Tools: Tools for processing data associated with species distribution modelling exercises. R package version 1.1-221. Available at CRAN.R-project.org/package=SDMTools. Accessed May, 2014.
93. Petoukhov V, et al. (2000) CLIMBER-2: A climate system model of intermediate complexity. Part I: Model description and performance for present climate. *Clim Dyn* 16(1):1–17.
94. Petoukhov V, et al. (2005) EMIC Intercomparison Project (EMIP–CO2): Comparative analysis of EMIC simulations of climate, and of equilibrium and transient responses to atmospheric CO2 doubling. *Clim Dyn* 25(4):363–385.
95. Greve R (1997) Application of a polythermal three-dimensional ice sheet model to the Greenland ice sheet: Response to steady-state and transient climate scenarios. *J Clim* 10(5):901–918.
96. Calov R, Ganopolski A, Claussen M, Petoukhov V, Greve R (2005) Transient simulation of the last glacial inception. Part I: Glacial inception as a bifurcation in the climate system. *Clim Dyn* 24(6):545–561.
97. Berger A (1978) Long-term variations of caloric insolation resulting from the earth's orbital elements. *Quat Res* 9(2):139–167.
98. Schneider von Deimling T, Held H, Ganopolski A, Rahmstorf S (2006) Climate sensitivity estimated from ensemble simulations of glacial climate. *Clim Dyn* 27(2-3): 149–163.
99. Oerlemans J (2005) Extracting a climate signal from 169 glacier records. *Science* 308(5722):675–677.
100. Intergovernmental Panel on Climate Change, ed. (2014) Information from paleoclimate archives. *Climate Change 2013: The Physical Science Basis* (Cambridge Univ Press, Cambridge, UK), pp 383–464.
101. Iakovleva L, Djindjian F, Maschenko EN, Konik S, Moigne A-M (2012) The late Upper Palaeolithic site of Gontsy (Ukraine): A reference for the reconstruction of the hunter–gatherer system based on a mammoth economy. *Quat Int* 255:86–93.
102. Starkovich BM, Stiner MC (2010) Upper Palaeolithic animal Exploitation at Klissoura Cave 1 in Southern Greece: Dietary Trends and Mammal Taphonomy. *Eurasian Prehistory* 7(2):107–132.
103. Starkovich BM (2012) Fallow deer (Dama dama) hunting during the Late Pleistocene at Klissoura Cave 1 (Peloponnese, Greece). *Mitteilungen Ges Für Urgesch* 21:11–36.